Angular Power Spectra of Anisotropic Stochastic Gravitational Wave Background: Developing Statistical Methods and Analyzing Data from Terrestrial Detectors

Deepali Agarwal

(In collaboration with Jishnu Suresh, Sanjit Mitra, Anirban Ain)

Belgian Dutch GW Meeting,
Oct 23-24, 2023

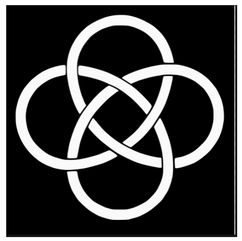

Agarwal et. al. Phys. Rev. D 108, 023011

Outline

- Motivation
- GW Radiometer Method
- Results

Gravitational Wave Sources

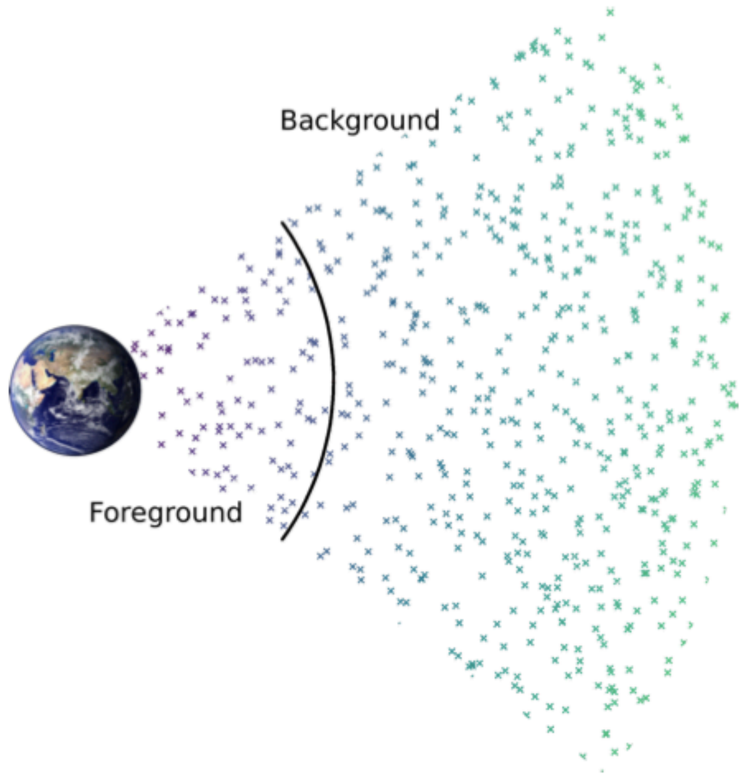

Alexander C. Jenkins

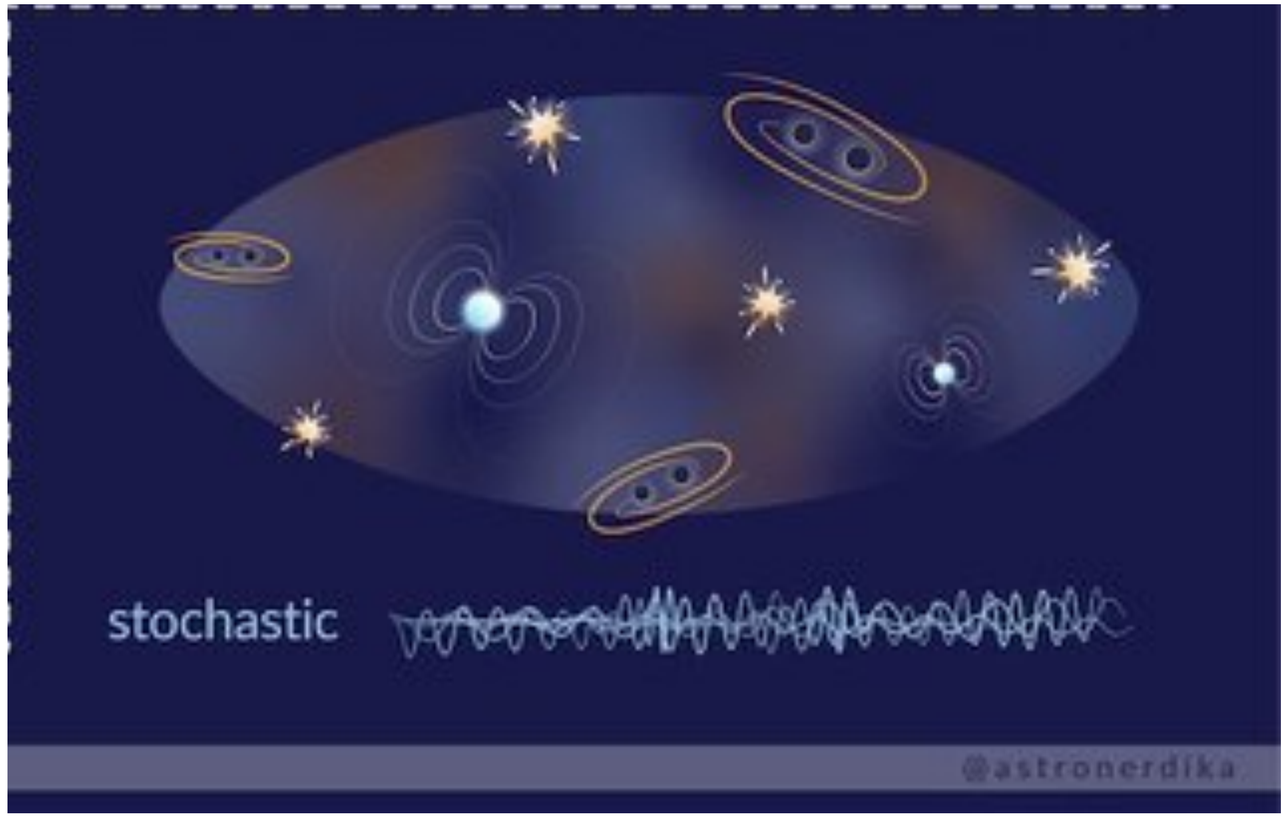

Source: https://www.spaceaustralia.com/news/cosmic-lighthouses-and-continuous-gravitational-waves

Is Intensity sky really isotropic?

Or Anisotropic ?

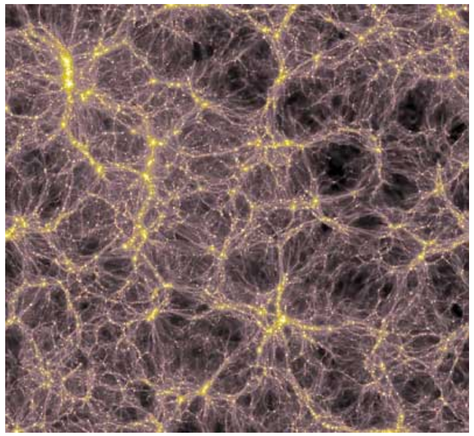

Specific distribution of galaxies in Cosmic Web

Credit: Volker Springel, Max Planck Institute for Astrophysics and Harvard-Smithsonian Center for Astrophysics, and Lars Hernquist, Harvard-Smithsonian Center for Astrophysics

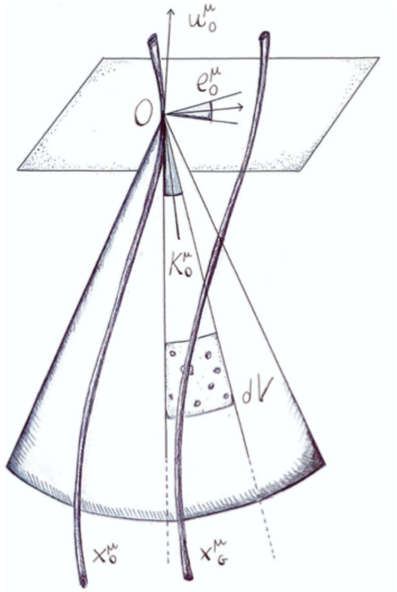

Anisotropy accumulated along with the line-of-sight

Cusin+ PRD 96, 103019 (2017)

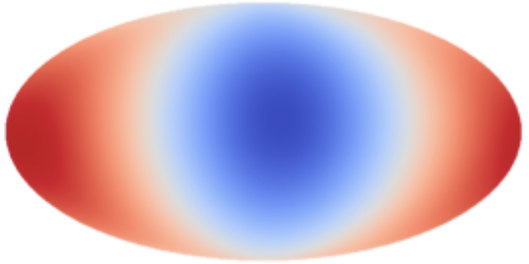

solar dipole

Dipole induced by the observer's peculiar velocity in cosmic rest frame

Credit: Chung et. al. Phys. Rev. D **106**, 082005

Ultimate Goal!!

Probing Anisotropy of SGWB at each frequency like CMB

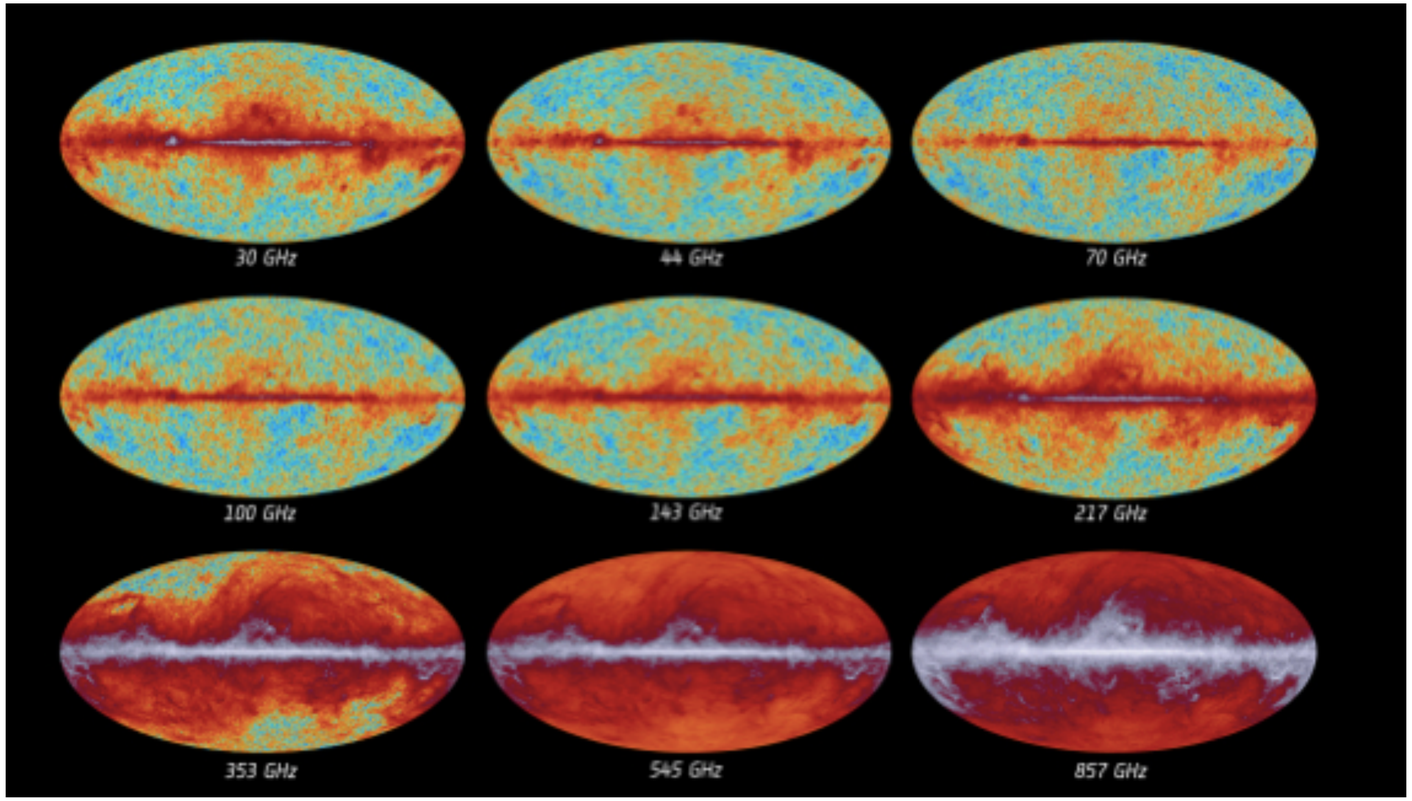

Credit: ESA and Planck Collaboration

Mapping Anisotropy with GW Radiometry

Cross-correlate data b/w non-colocated detectors with optimal filtering.

Mitra et. al. 2008

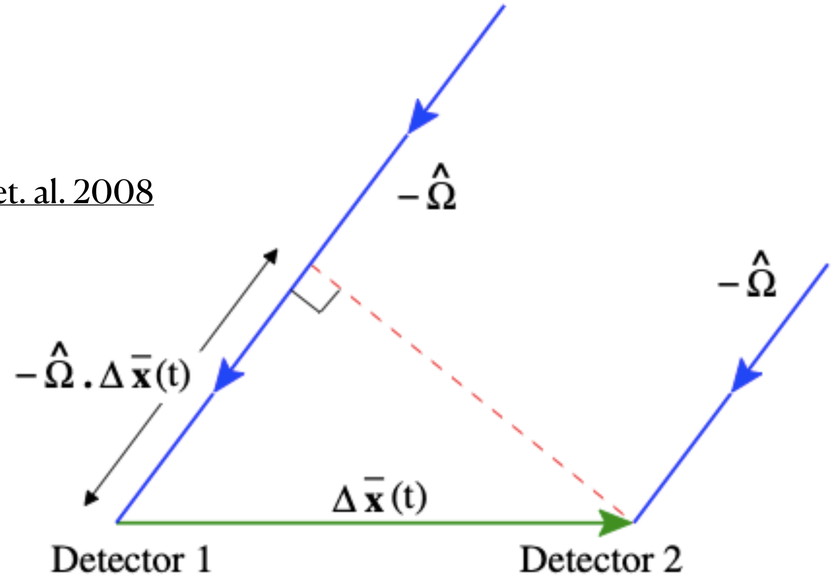

FIG. 1 (color online). Geometry of an elementary radiometer. Above, $\mathbf{\Delta x}(t)$ is the separation or baseline vector between the two detectors; as the Earth rotates, its direction changes, but its magnitude remains fixed. The direction to the source $\hat{\mathbf{\Omega}}$ is also fixed in the barycentric frame. The phase difference between signals arriving at two detector sites from the same direction is also shown.

Folding the whole observation run data to one sidereal day.

Ain et. al. 2015

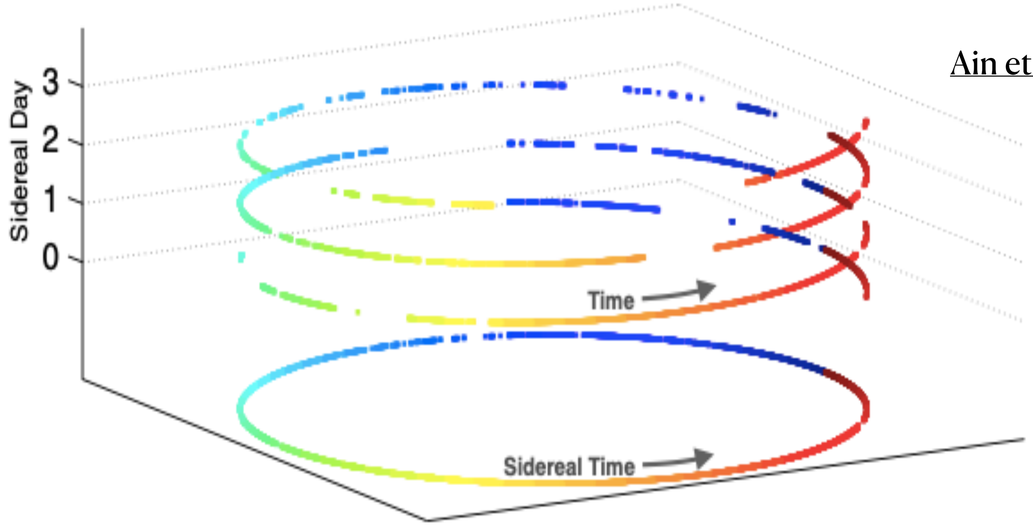

Example of observed sky

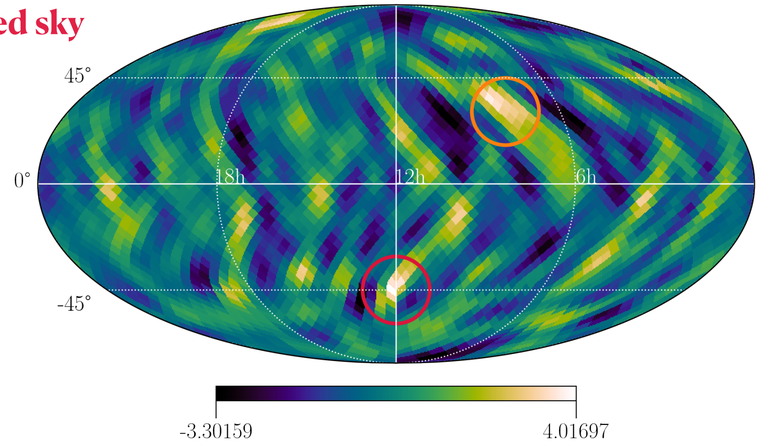

Agarwal et. al. 2021

Narrowband Angular Power Spectrum

Suitable statistic to characterise Statistically Isotropic Gaussian Background

Unbiased estimator of the narrowband angular power spectra

$$\hat{C}_\ell(f) = \frac{1}{2\ell+1} \sum_m \left[|\hat{\mathscr{P}}_{\ell m}(f)|^2 - \left[\Gamma'^{-1}\Gamma\Gamma'^{-1}\right]_{\ell m,\ell m}(f) \right]$$

Results

O3 HLV , f = [20, 1726] Hz, Δf= 1 Hz, $\ell_{\max}$ =15

- Using Folded data and PyStoch-SpH pipeline
- We produce data for $\ell_{\max}$=30, only invert the matrix with $\ell_{\max} = \dfrac{\pi f(\mathrm{Hz})}{50}$
- But the angular power spectrum from clean map has correlated modes

Correlated Harmonic Modes

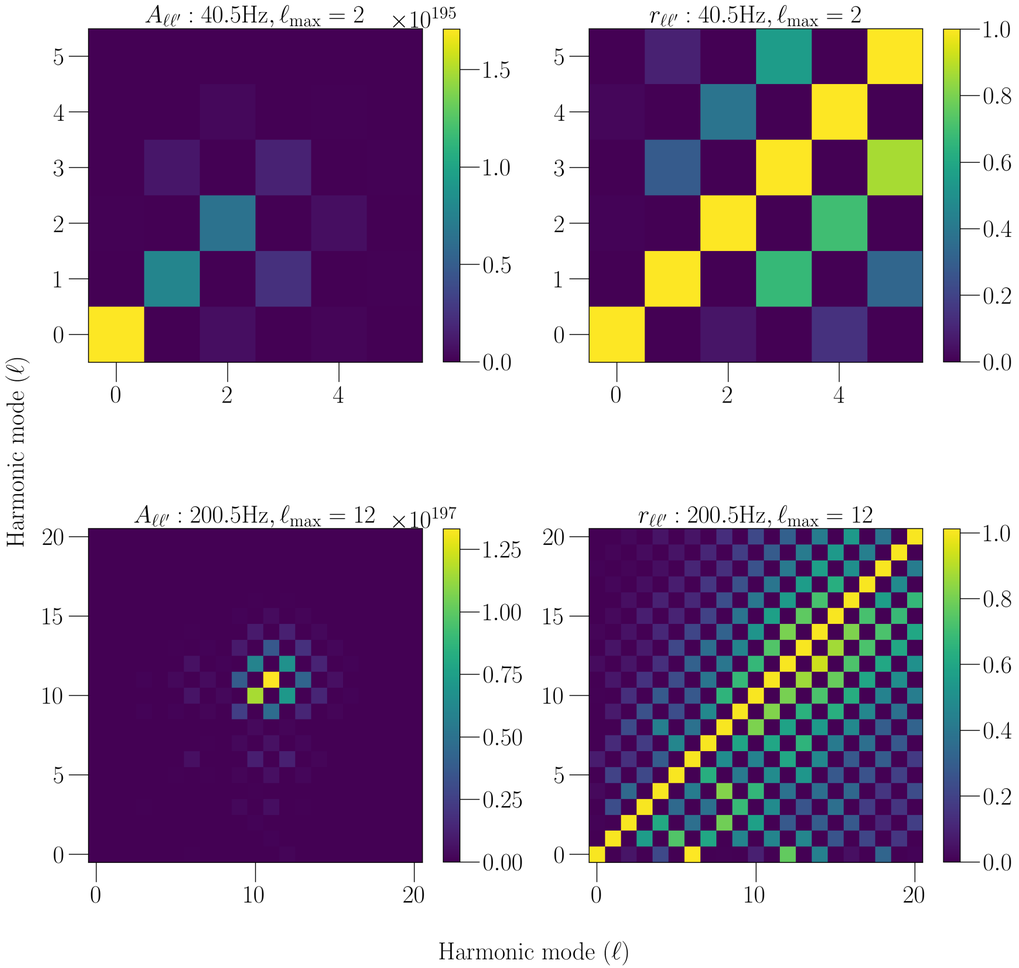

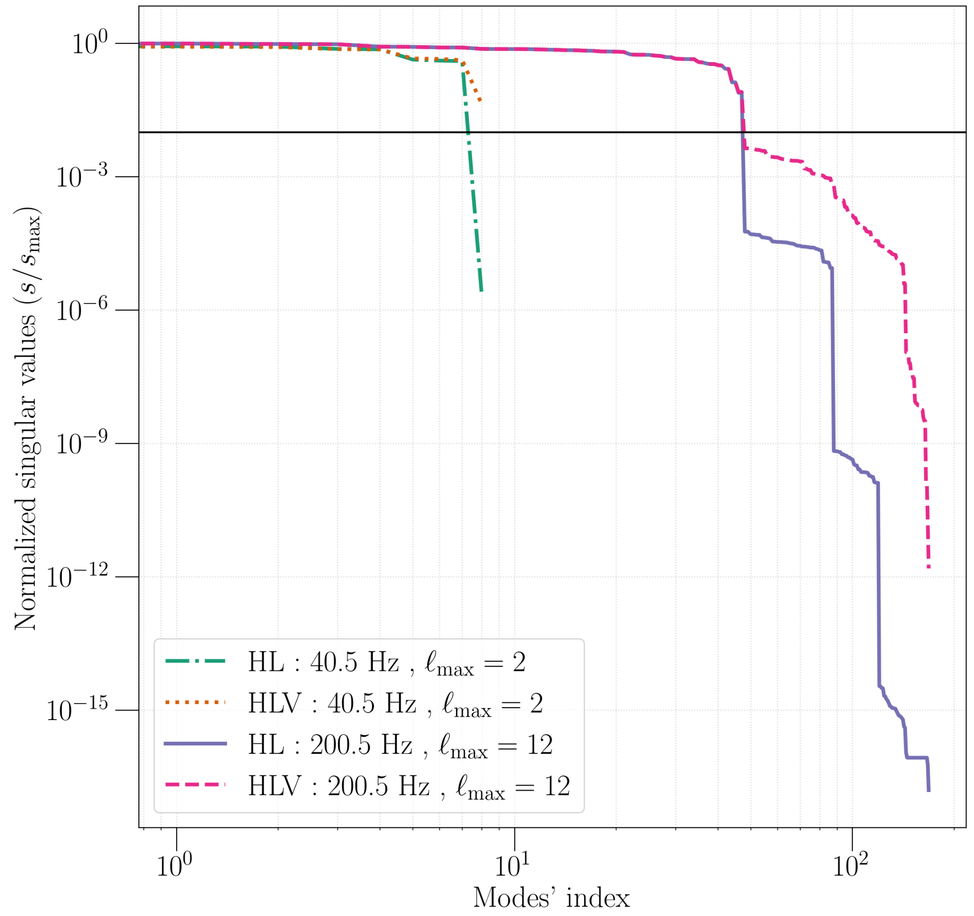

Results

Significance

- The zero lag data is almost consistent with the time shifted data.
- Approximated pdf for SNR in noise only case

$$P(y = \rho_\ell(f)) = \sqrt{2k}\,\chi^2_k(y\sqrt{2k} + k)$$

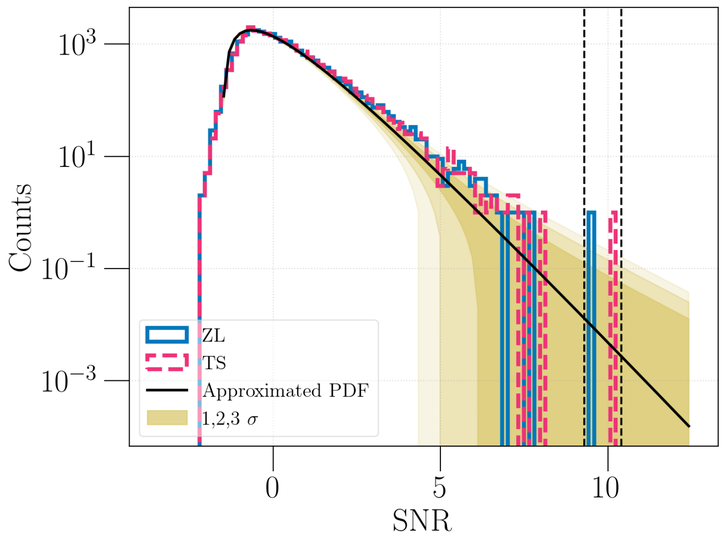

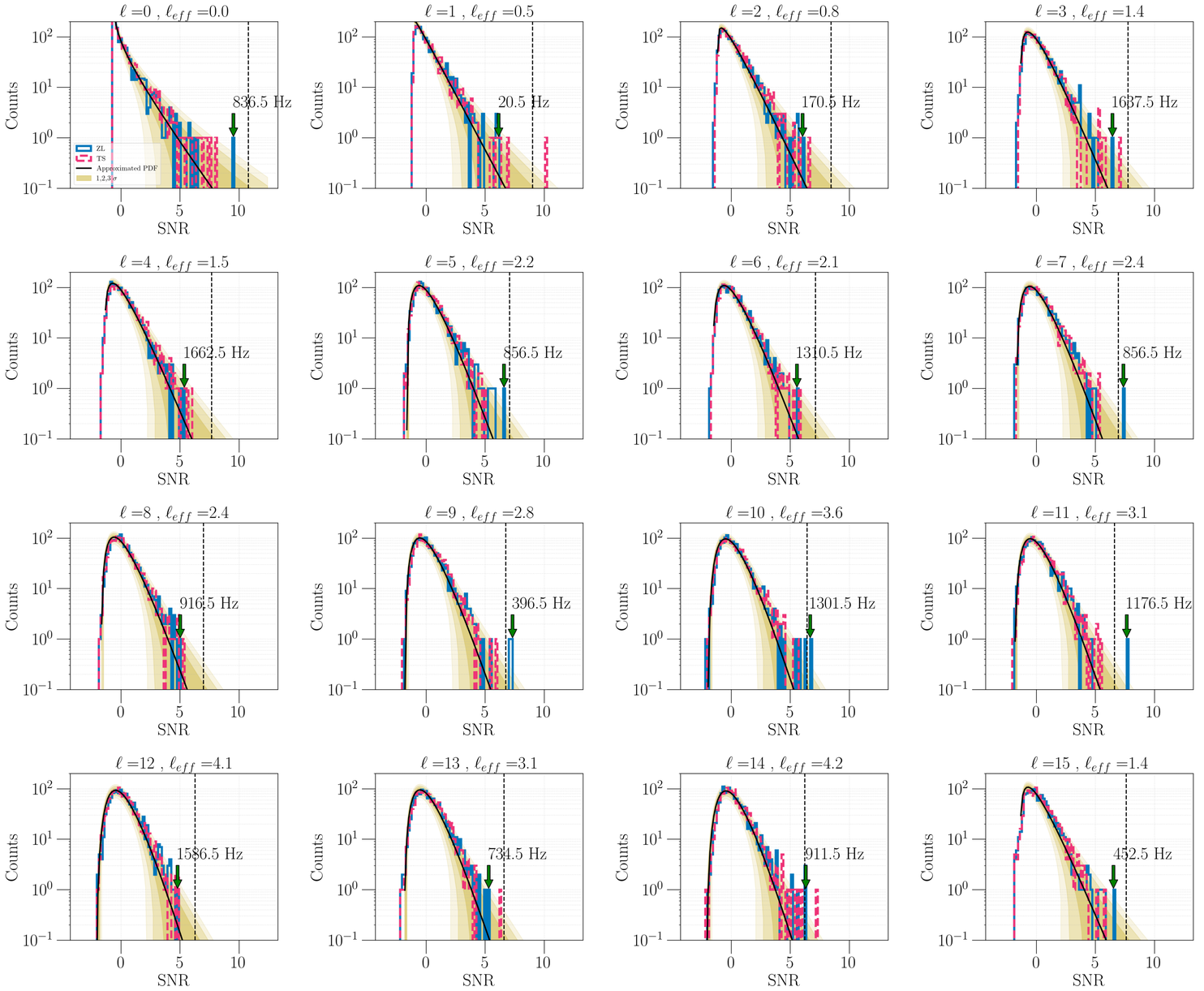

Results

Bayesian Upper Limit, $(C_l^{95\%})^{1/2}$

- The analytical expression of the likelihood for is C_l non-trivial due to colored correlated noise.
- Monte Carlo sampling and marginalized over calibration uncertainty
- 95% upper limit range :

  $3.1 \times 10^{-9} - 0.76\ \mathrm{sr}^{-1}$

- Our upper limits at 65 Hz, $8.4 \times 10^{-8} \leq C_\ell^{1/2} \leq 7.6 \times 10^{-8}\ \mathrm{sr}^{-1}$ are higher than the predicted anisotropy (Capurri et. al. 2021) $3.2 \times 10^{-14} \lesssim C_\ell^{1/2} \lesssim 4.5 \times 10^{-14}\ \mathrm{sr}^{-1}$ by several of orders.
- As the detector network grows with improved sensitivity, we may be able to detect the anisotropy with the third-generation detectors such as the Einstein Telescope. (Mentasti et. al. 2021)

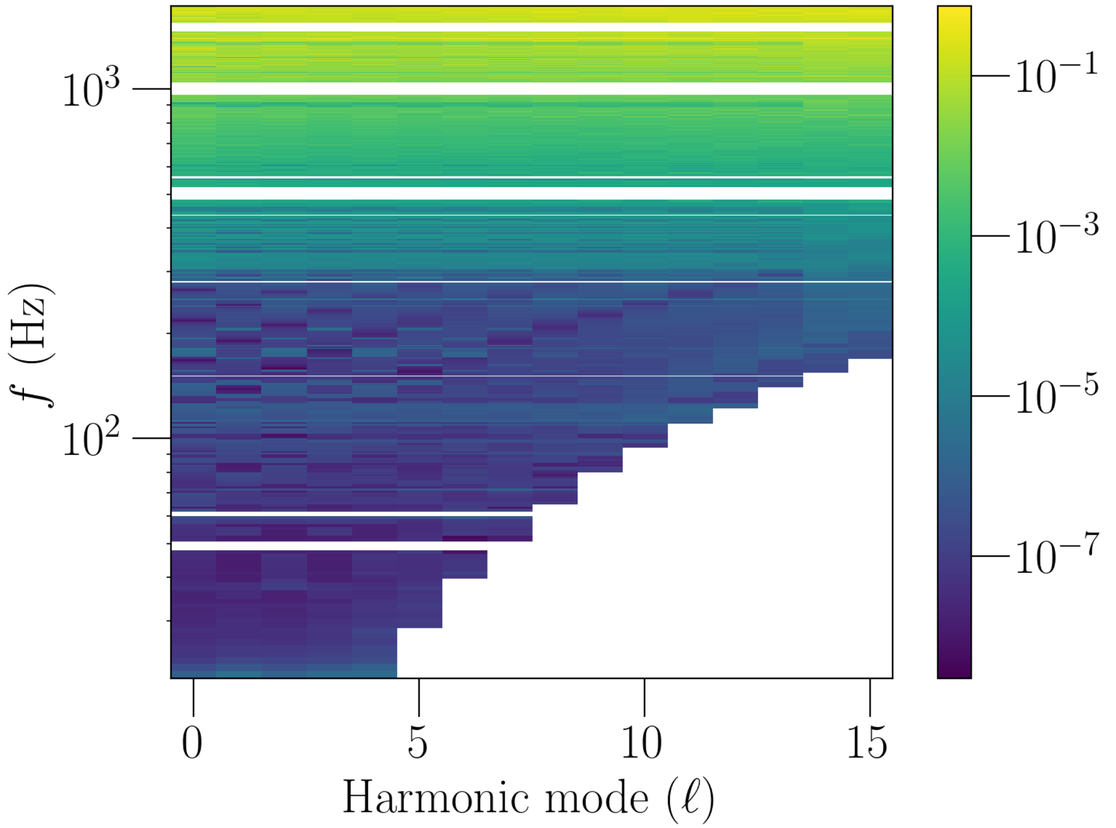

Summary

- We have performed an unmodeled search for narrowband anisotropic (extended) background in the spherical harmonics basis.
- The data is found to be consistent with the noise. Hence we set the bayesian upper limit $C_l^{95\%}(f)$.
- The estimators can be used to constrain the models which predicts the non-power frequency spectrum.
- The analytical expression of the likelihood for C_l can be further explored.
- Detection efforts are growing up and sensitivity of data is increasing.

Credit: LVK collaboration

Detection is on horizon !!

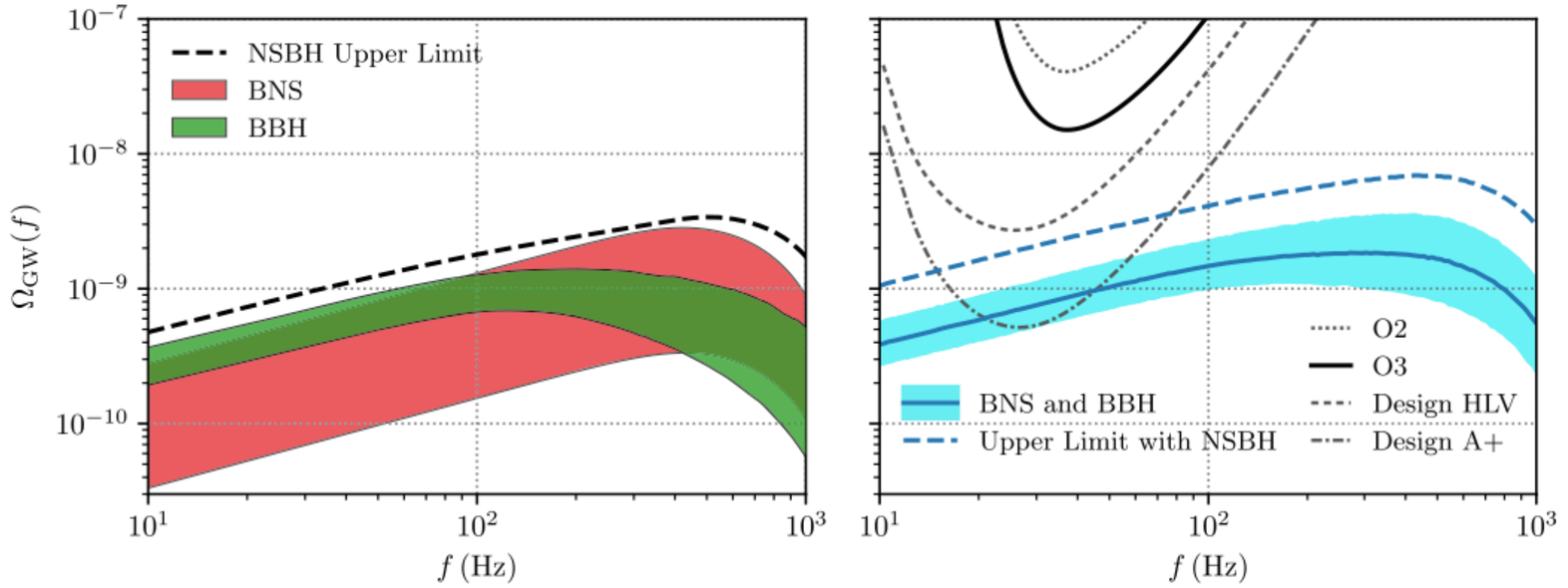

FIG. 5. Fiducial model predictions for the GWB from BBHs, BNSs, and NSBHs, along with current and projected sensitivity curves. In the left panel we show 90% credible bands for the GWB contributions from BNS and BBH mergers. Whereas the BNS uncertainty band illustrates purely the statistical uncertainties in the BNS merger rate, the BBH uncertainty band additionally includes systematic uncertainties in the binary mass distribution, as described in the main text. As no unambiguous NSBH detections have been made, we only show an upper limit on the possible contribution from such systems. The right panel compares the combined BBH and BNS energy density spectra, and 2σ power-law integrated (PI) curves for O2, O3, and projections for the HLV network at design sensitivity, and the A + detectors. The solid blue line shows the median estimate of $\Omega_{\rm BBH+BNS}(f)$ as a function of frequency, while the shaded blue band illustrates 90% credible uncertainties. The dashed line, meanwhile, marks our projected upper limit on the total GWB, including our upper limit on the contribution from NSBH mergers.

Extra Slides

Method

Dirty map

$$X_{\ell m}(f) = \sum_{\mathcal{J}t} \frac{\gamma^{I*}_{ft,\ell m} C^{\mathcal{J}}(t;f)}{P_{\mathcal{J}_1}(t;f) P_{\mathcal{J}_2}(t;f)}$$

Fisher information matrix

$$\Gamma_{\ell m,\ell' m'}(f) = \sum_{It} \frac{1}{P_{\mathcal{J}_1}(t;f)\, P_{\mathcal{J}_2}(t;f)} \gamma^{I*}_{ft,\ell m} \gamma^{I}_{ft,\ell' m'}$$

Regularised Fisher information matrix

$$\Gamma'^{-1}(f) = US'^{-1}U*$$

Clean map

$$\hat{\mathscr{P}}_{\ell m}(f) = \Gamma'^{-1}_{\ell m,\ell m}(f)\,.\,X_{\ell m}(f)$$

Standard deviation of each multipole for above estimator

$$\sigma_{\ell m}(f) = \sqrt{\mathrm{Var}[\hat{\mathscr{P}}_{\ell m}(f)]} = \sqrt{\left[\Gamma'^{-1}(f)\,\Gamma(f)\,\Gamma'^{-1}(f)\right]_{\ell m,\ell m}}$$

Unbiased estimator of the narrowband angular power spectra

$$\hat{C}_\ell(f) = \frac{1}{2\ell+1} \sum_m \left[|\hat{\mathscr{P}}_{\ell m}(f)|^2 - \left[\Gamma'^{-1}\,\Gamma\,\Gamma'^{-1}\right]_{\ell m,\ell m}(f) \right]$$

Standard deviation of the angular power spectra estimator

$$\sigma_{C_\ell}(f) = \sqrt{\frac{2}{(2\ell+1)^2} \sum_m |\sigma_{\ell m}(f)|^2}$$

Signal to noise ratio

$$\mathrm{SNR} = \frac{\hat{C}_\ell(f)}{\sigma_{C_\ell}(f)}$$

Results

O3 HLV , f = [20, 1726] Hz, Δf= 1 Hz, $\ell_{\max}$ =15

- Using Folded data and PyStoch-SpH pipeline
- We produce data for $\ell_{\max}$=30, only invert the matrix with $\ell_{\max} = \dfrac{\pi f(\mathrm{Hz})}{50}$
- $$\mathbf{B}(f) \equiv B_{\ell\ell'}(f) = \frac{2}{(2\ell+1)(2\ell'+1)} \sum_{m,m'} |\Gamma|^2_{\ell m,\ell' m'}(f)$$
- But the angular power spectrum from clean map has correlated modes
- Covariance matrix for $\hat{C}_\ell(f)$
- $$\mathbf{\Sigma}(f) \equiv \Sigma_{\ell\ell'}(f) = \frac{2}{(2\ell+1)(2\ell'+1)} \sum_{m,m'} |\Gamma'^{-1}\Gamma\Gamma'^{-1}|^2_{\ell m,\ell' m'}(f)$$

Can we derive broadband angular power spectrum from narrowband estimators?

- If we assume $\hat{\mathbf{C}}(f) \equiv \hat{C}_\ell(f)$ is a random vector which obeys the multivariate Gaussian distribution with covariance matrix $\mathbf{\Sigma}(f)$. then joint PDF (log likelihood) using the estimator $\hat{\mathbf{C}}_\ell(f)$ from multiple frequency bin is given as

$$-2\,ln\,L = \sum_f \left[\hat{\mathbf{C}}(f) - w^2(f)\,\mathbf{C}\right] . \mathbf{\Sigma}^{-1}(f) . \left[\hat{\mathbf{C}}(f) - w^2(f)\,\mathbf{C}\right]$$

- The maximum likelihood estimator for the broadband angular power spectrum $\mathbf{C}$

$$\hat{\mathbf{C}} = \left(\sum_f w^4(f)\,\mathbf{I} . \mathbf{\Sigma}^{-1}(f) . \mathbf{I}\right)^{-1} \left(\sum_f w^2(f)\,\mathbf{I} . \mathbf{\Sigma}^{-1}(f) . \hat{\mathbf{C}}(\mathbf{f})\right)$$

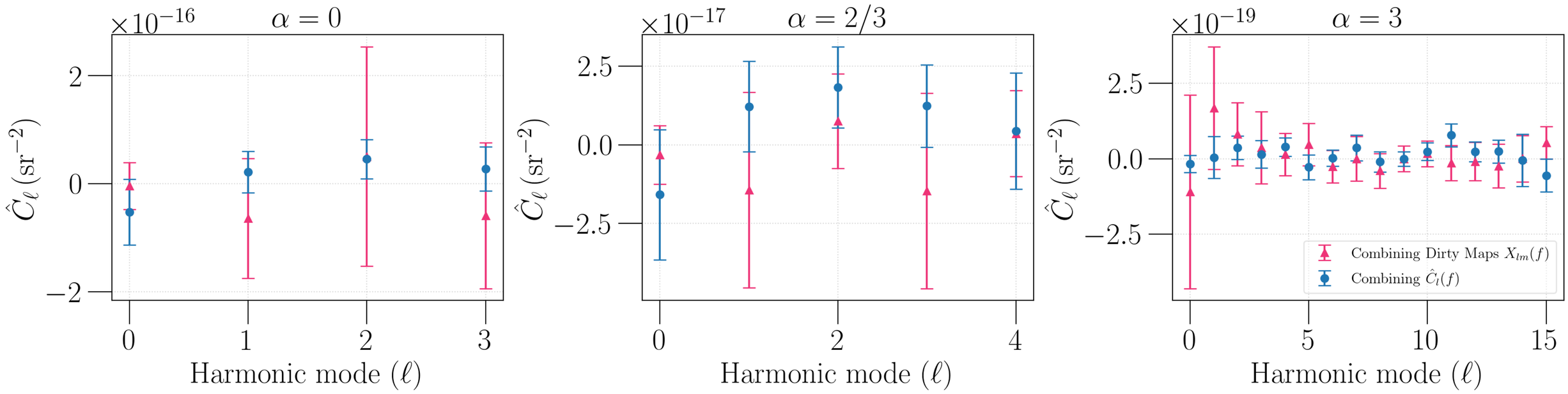
$\alpha = 0$
$\times 10^{-16}$
$\hat{C}_\ell\,(\mathrm{sr}^{-2})$
2
0
−2
0
1
2
3
Harmonic mode (ℓ)
$\alpha = 2/3$
$\times 10^{-17}$
$\hat{C}_\ell\,(\mathrm{sr}^{-2})$
2.5
0.0
−2.5
0
2
4
Harmonic mode (ℓ)
$\alpha = 3$
$\times 10^{-19}$
$\hat{C}_\ell\,(\mathrm{sr}^{-2})$
2.5
0.0
−2.5
0
5
10
15
Harmonic mode (ℓ)
Combining Dirty Maps $X_{lm}(f)$
Combining $\hat{C}_l(f)$